A micro-device integrating vertical and bottom electrodes for 3D cell rotation

Prateek Benhal

University of Canterbury, Christchurch, Private Bag 4800, New Zealand,
AgResearch Ruakura Research Centre, East Street, Private Bag 3115, Hamilton 3240, NewZealand

Abstract. We report a Lab-on-chip micro device for rotating a spherical object such as bovine cell in three dimensional (3D) spaces. Micro device consists of two pairs of orthogonal vertical wall electrode along with bottom transparent indium tin oxide (ITO) electrodes. Photolithography technique is employed to fabricate bottom part of the micro device. On the other hand micro milling is applied to fabricate the top electrodes of 500 µm height. The entire device is only 75X25 mm in length and width upon which particle rotation is achieved. Micro device works entirely on this dielectrophoresis (DEP) phenomenon to rotate the cell in 3D spaces. Rotating fields are optimized through simulation and results are presented along with analysis. The experiments are carried out to determine the cell rotation rate. Rotation of cell in 3D spaces has its unique advantages in automation of high throuput mammalian cloning procedures. Cloning procedures such as enucleation requires a cell to be rotated in 3D spaces for genetic material extraction. Enucleation also requires the cell to be precisely rotated and controlled. This precise rotation control is achieved by electrorotation through DEP.

Keywords: DEP, electrorotation, micro-device, micro-milling.
PACS: 85.50.-n

I. INTRODUCTION

There is an enormous interest in development of micro devices for cell manipulation studies such as cell sorting, cell characterization and cell rotation [1][2][3]. Advent of these micro-devices through the application of dielectrophoresis (DEP) phenomenon has facilitated high-throughput cell manipulation techniques. In DEP non uniform electric field is generated [4]. This field polarizes any neutrally charged particles. DEP force is also generated on the polarized particle to levitate, translate, orient and rotate with respect to electric field direction and strength [5][6]. According to theory, DEP force is proportional to square of the electric field strength. To obtain DEP force on the particle various combinations of electrode designs have been proposed over the past decade including planar designs such as Interdigitated electrode array (IDA) [7], polynomial design [8] and castellated designs[9].

This paper presents a micro-device comprising 3D electrode structures for cell sorting, and rotation studies on micron sized particles based on DEP phenomenon. Recently optical electronic tweezers (OET) are employed to rotate cells in pitch axis [10]. Our device function similar to OET however, works only on DEP. Our micro device can even rotate particle in all the three axes such as yaw, pitch and roll. Micro device fabricated is simple in design and also cost effective as compared to OET. The micro-device consists of aligning and integrating two pairs of orthogonally arranged vertical electrode structure of 500µm height on top of bottom ITO electrode substrate. Vertical electrodes are micro-milled on Perspex substrate. One can control the rotation of particle by controlling the electrical signals. If vertical electrodes are applied with AC along with 90˚ shift, the particle will rotate in yaw, and if vertical electrodes are grounded and bottom electrodes are activated we witness pitch axis rotation. From Euler angles it has been shown that one can obtain 3D rotations by rotating a sphere in any of the two axes [11][12].

DEP fields are generated by applying AC voltage on bottom electrodes and also on the vertical electrodes depending upon the desired sequence of rotation direction. Only one particle is suspended at the center of the rotation chamber along with a buffer solution. Initially solid polystyrene beads of different sizes are used to obtain the desired rotation for preliminary set of experimental validation of the device along with simulation results. Later bovine cells of 120 micron diameter are suspended and tested for rotation in DEP field. Experimental results are presented along with simulation results in COMSOL v4.3 and Matlab software.

II. THEORETICAL BACKGROUND

DEP is a phenomenon in which force is exerted on a neutrally charged dielectric particle under the influence of non-uniform electric fields. Different order and shapes of electrodes are designed to obtain fields to induce dipoles in the particle and these dipoles polarize the neutrally charged particles. Any particle under the influence of electric field exhibit DEP. However, the strength of the DEP force on the particle strongly depends upon the electrical properties of the particle and the surrounding medium, on the particle shape and size, and also on the frequency of the applied field. Fields of particular frequency can manipulate and rotate cells and particles with enormous selectivity. This also increases the chances of selectively separating the cells and rotating them at required precision.

The time-averaged DEP force for a spherical dielectric particle from the interaction of non uniform field is given by,

$$F_{DEP} = 2\pi\varepsilon_m r^3 Re(f_{cm})\nabla E^2 \qquad (1)$$

Where, ε_m is the permittivity of surrounding medium, r is the particle radius, f_{cm} is the Clausius-Mossotti (CM) factor, and E is the root mean square value of the electric field.

However, torque is induced on the particle for electrorotation which occurs from the result of superimposition of electric fields on a particular area within the workspace [13]. This workspace composed of optimized spacing between the electrodes along with suitable AC field. Rotation also depends upon the polarizability of the particle with the surrounding medium [14]. The DEP electric torque generated by polarizing the particle in AC field is given by,

$$T_{DEP} = -4\pi r^3 \varepsilon_m Im(f_{cm})E^2 \qquad (2)$$

Where, f_{cm} is the imaginary part of CM and E is the magnitude of electrical field strength.

Verification of DEP Torque

DEP is further classified by directions. If the force on the particle is in the same direction as the electric field gradient, it is termed as positive DEP. If the force repels the particle away from the region of higher electrical field gradient, then it is termed as negative DEP. Each of these methods has its own unique applications. Particle experiencing positive or negative DEP is dependent upon the polarizability of the particle with the surrounding medium. If the polarizability is less than that of the medium the particle rotates in the anticlockwise if not in clockwise direction. Polarizability is a complex function dependent not only upon the properties of the particles and the surrounding medium but also on the applied field frequency. Particles experience different DEP rotation speed depending upon the frequency of the applied field.

In other words, DEP rotation, to be applied on the particle in the rotation chamber, takes place when $Im(f_{cm})$ of the CM exhibits either one or two frequency spectrum peaks against applied frequency of the AC field. Peaks represent the direction of rotation of the particle. Eq. 3 provides a method to calculate CM factor for the known parameters of particle and its surrounding medium.

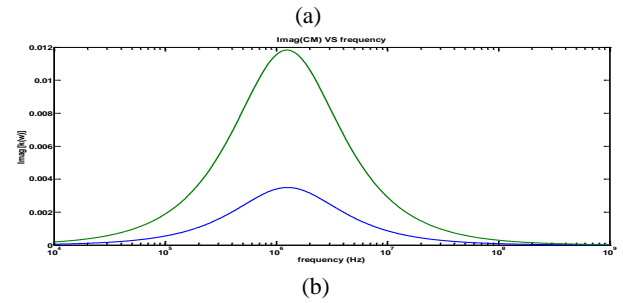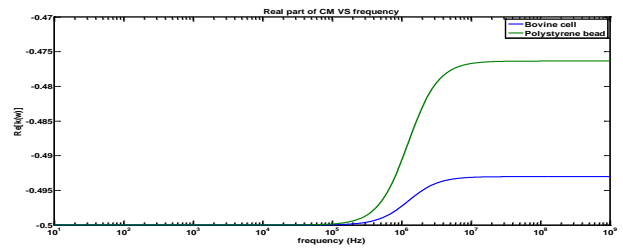$$f_{cm} = \frac{\varepsilon_p^* - \varepsilon_m^*}{\varepsilon_p^* + 2\varepsilon_m^*} \qquad (3)$$

Where, ε^* is the dielectric constant and is dependent upon the conductivity(σ) , and angular frequency (ω) as,

$$\varepsilon^* = \varepsilon - \frac{\sigma}{j\omega} \qquad (4)$$

j denotes an imaginary number.

TABLE 1. Parameter constant of particle and medium

| Item	Dielectric constant(ε)	Conductivity (σ) S/m
Polystyrene	2.5	1.00E-16
Bovine cell	0.73	1.8E-14
DI Water	78	5.00E-03

(a)

(b)

FIGURE 1: Frequency dependency of particle rotation on complex conductivity and permittivity factors of cell and the surrounding medium. Table 1 is used as a reference to obtain

these plots. (a). Real part of CM factor (b) Imaginary part showing a positive peak, indicating particle rotation in clockwise direction. Negative peak indicates particle rotation in anticlockwise direction.

Cell Rotation condition

Figure 2 shows the basic design concept of the micro device for 3D electro rotation and the acting torque analysis of the particle. The rotational torque is applied simultaneously on the particle by switching the AC signals. Since DEP force and torque are proportional to cubic r, it implies that bigger the radius of particle larger will be the forces acting on it and also the rotation chamber has to be calibrated to support the rotation of bigger sized particles such as bovine cells. Finally we can conclude that the device can support to rotate the particles of sizes ranging between 1-60 micron radius particles sufficiently depending upon the applied field.

(a)   (b)
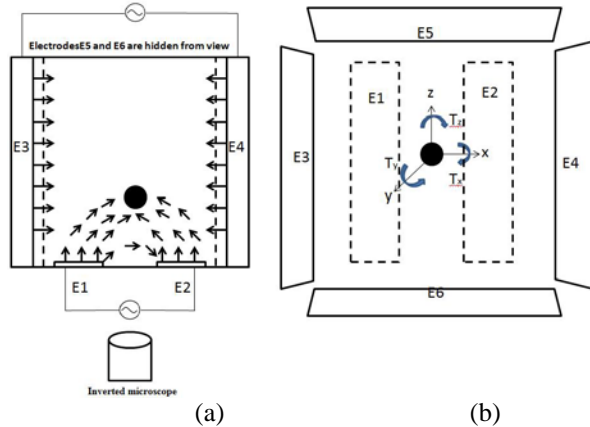
FIGURE 2: Basic design concept of the device for particle/cell rotation studies (**Not to scale**). E1 and E2 as bottom ITO electrodes, and E3, E4, E5, and E6 representing vertical side wall electrodes made of brass. (a). Side view of the device. Arrow represents not to scale electric field direction. (b). Rotational torques acting on the particle.

III.   SIMULATION

Before carrying out fabrication process, simulation results provide an efficient tool to optimize the devise design. Using finite element analysis (FEA) one can determine the electrical field strength required to develop the rotational torque on the particle. Researchers found in the past that about 10^3-10^5V/m field strength is required to rotate cells or particles of 1-60µ radius [15]. To achieve this, a suitable rotational work space is required to suspend and rotate particle in the rotation chamber in yaw, pitch and roll axis.

Through electric field parametric simulations, it has been found that the rotation chamber is suitable at

750 µm in width and Length. Moreover, height of vertical electrode is optimum at 500 µm and width of the bottom ITO electrodes found to be 250 µm wide and with 30 µm gaps. A bottom electrode of 200 nm thickness is considered.

Electrical field is generated in COMSOL v4.3 software and the data points are analyzed in Matlab 2011b. Governing equation (5) and (6) is used for electric field simulations.

$$E = -\nabla v \qquad (5)$$

$$\nabla(D) = \rho_V \qquad (6)$$

Where, E is the electric field which is dependent upon the time dependent AC voltage potential$v$. D is the electric field displacement and is calculated by charge distribution inside the material; in our case this will be negligible because we are concerned on the surface charges. For simulations, material properties are defined for liquid water domain with suitable conductivity and permittivity as shown in Table 1. Vertical wall electrode domains are defined as brass and bottom electrodes as ITO. Particle is not considered for current electrical field simulations, this is because by simulating suitable rotational fields at the center region one can rotate any spherical object provided with suitable field strength. However, our immediate future vision is to simulate a real world rotating 3D cell in DEP field. Simulations are divided into two categories, one for yaw axis and other for analyzing pitch axis rotational fields.

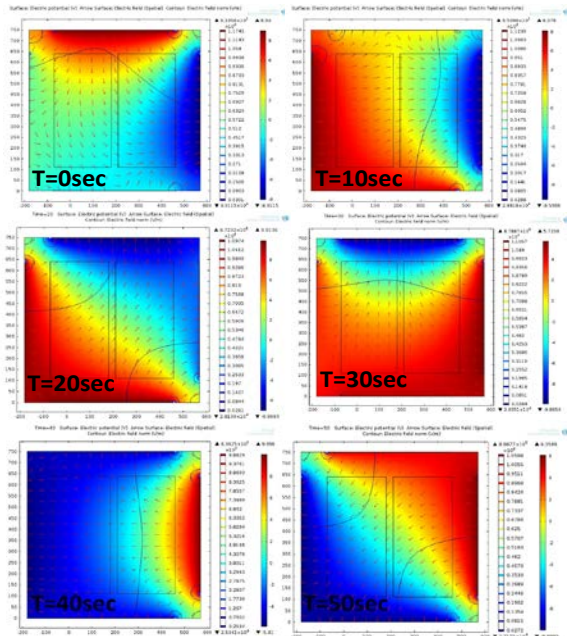### *Yaw axis electric field simulation*

A 2D model is built in COMSOL v4.3 software for simulation for analyzing yaw axis rotational fields. Figure (2b) is considered for this study and it represents top view of the model as shown in Figure 3. A fine mesh is generated for finite element analysis (FEA) with a maximum element size of 39.8 µm consisting of 32550 elements.

(a)   (b)
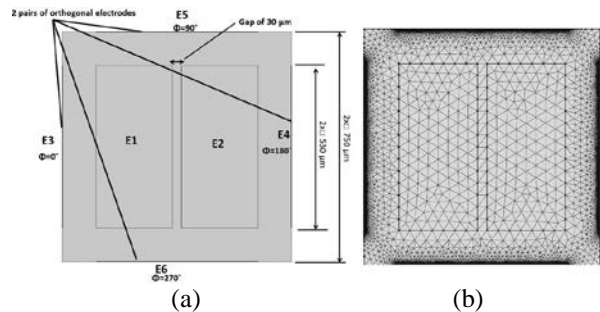
FIGURE 3: Shows a basic model built in COMSOL for FEA. (a) Shows the top view of the model along with micron

scale dimensions. (b) A generated mesh in COMSOL. The finer the mesh finer will be the data points for analysis.

Figure 4, shows a 0-50 second's time varying electrical potential and field simulation with 10 second step period. Sinusoidal voltage of 90˚ phase shifts is applied at the two pairs of orthogonal electrodes along with 100 kHz frequency. It is found that only the phase shift plays a key role as compared to time varying field directions. Moreover, at the center region for yaw axis rotation of cell at constant magnitude is found showing fields have linearly superimposed onto each other.

FIGURE 4: Electric field simulation in V/m representing electric potential color image with contour plot of electric field arrow. Legends represent intensity of change in voltage and varying fields.

To show the rotational fields, electric field normalized vector arrows are plotted as shown in Figure 5. With the change in time and phase, field rotates and makes 360˚ rotation and is very much evident near the center chamber.

Matlab plots in Figure 6 shows high resolution plots of 10 by 10 microns at the center of the chamber to determine the change in electric fields. It is found that even though fields are rotating in yaw axis only 5% standard deviation of the rotational field is found in the electric field magnitude.
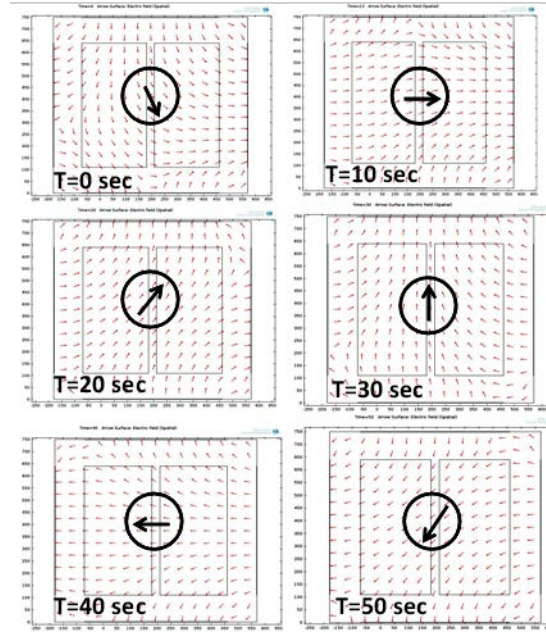
FIGURE 5: Shows normalized arrow plots. At the center of the chamber rotational arrows are marked for clarity.
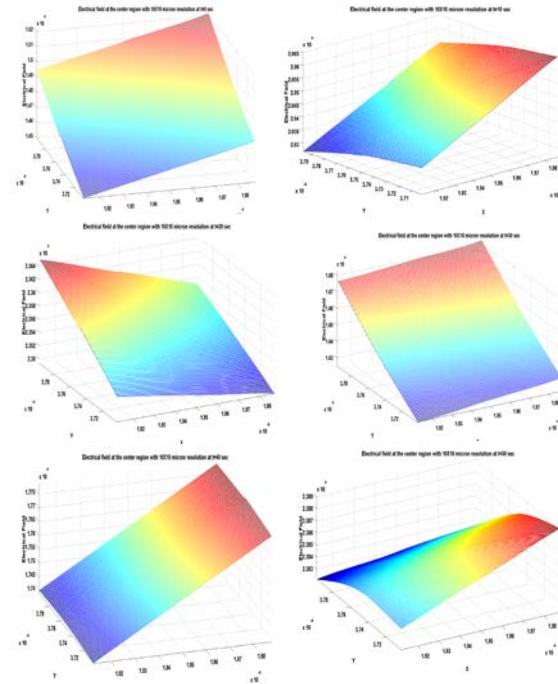

FIGURE 6: 10x10 micron high resolution plot of corresponding electrical field from Figure 4. Magnitude of field at the center is found to be between $2x10^4$ V/m to $3x10^4$ V/m.
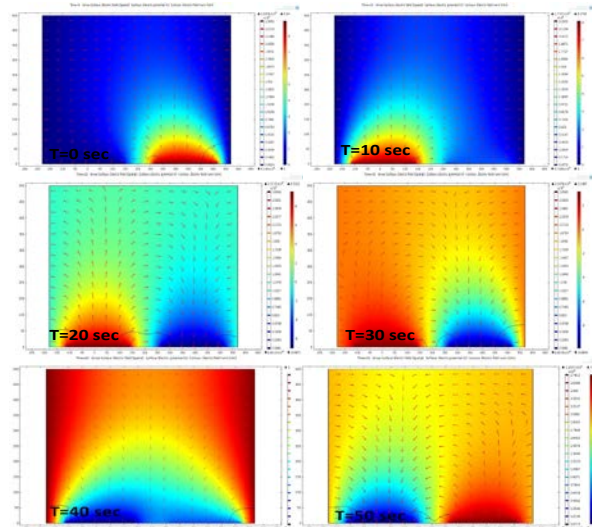
Pitch axis electric field simulation

Next step involves analyzing pitch axis rotational fields. Figure (2a) is considered for this study and it

represents side view of the model as shown in Figure 7. A fine mesh is generated for FEA with a maximum element size of 27.8 µm consisting of 37394 elements.


(a)   (b)
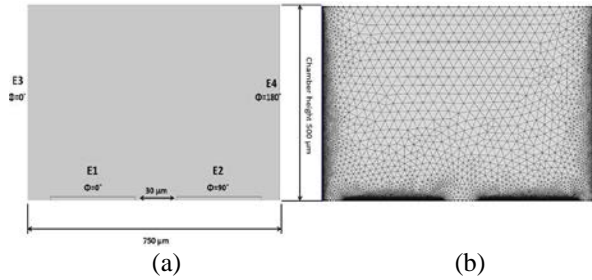
FIGURE 7: Shows a basic model built in COMSOL for FEA. (a) Shows the side view of the model along with micron scale dimensions. Bottom electrode material is considered as ITO with 250 micron width and 200 nm height. (b) A generated mesh in COMSOL. The finer the mesh finer will be the data points for analysis.

Figure 8, shows time varying electric potential simulation at 10 volts peak to peak AC voltage with 90˚ phase shift at bottom electrodes. The side wall electrodes are grounded for pitch axis rotation. Electric field contour and arrows plots generate $10^3 - 10^4$ V/m rotational field at the center chamber.


FIGURE 8: Electric field simulation in V/m representing electric potential color image with contour plot of electric field arrow. Legends represent intensity of change in voltage and varying fields.
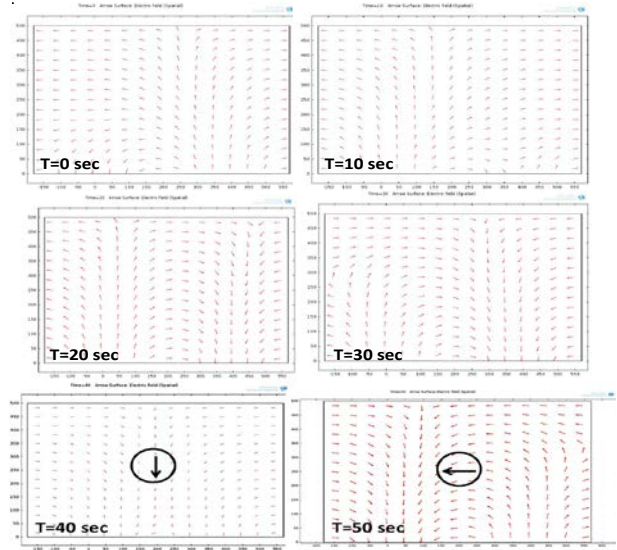
FIGURE 9: Shows normalized arrow plots. At the center of the chamber rotational arrows are marked for clarity.

Matlab plots in Figure 10 shows high resolution plots of 10 by 10 microns at the center of the chamber to determine the change in electric fields. It is found that even though fields are rotation in yaw axis only 5% of standard deviation of the rotational field is found in the electric field magnitude.
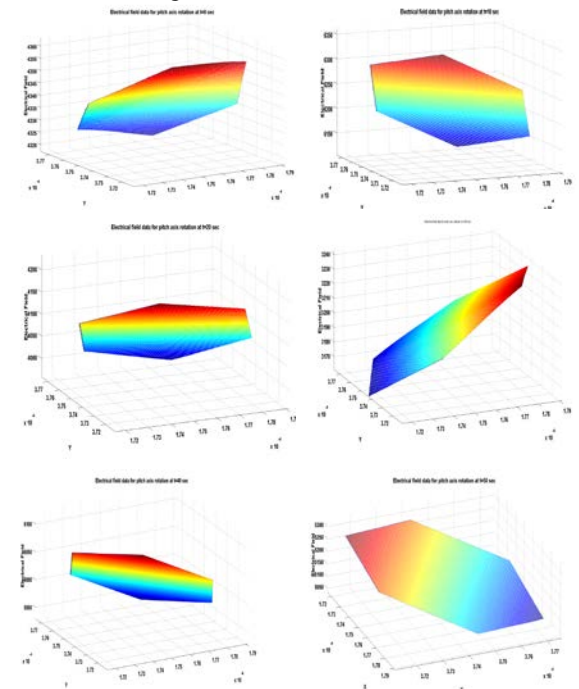

FIGURE 10: 10x10 micron high resolution plot of corresponding electrical field from Figure 4. Magnitude of field at the center is found to be between $4x10^3$ V/m to $5x10^3$ V/m.

From the simulation results rotating electric fields generated can rotate a particle in 3D space according to theory of dielectrophoresis and electrorotation. However, fabricating a micro device needing 500 µm thick metal using photolithography techniques such as electroplating technique is highly impossible. Hence, a micro-milling device is employed to fabricate the device we have designed and simulated. Following section talks about the fabrication procedure and micro device prototype.

# IV. DEVICE FABRICATION

A. Size of micro device

The micro device is made up of two stages of fabrication procedures. First stage involves depositing and patterning indium tin oxide (ITO) electrodes on top of a glass wafer as the bottom electrode. The patterned ITO electrode is 200 nm in thickness, 25mm in width and 75mm in length as shown in Figure 11. The gap between two ITO electrodes is kept at 30µm. Insulating layer such as zinc oxide is coated on top of these electrodes. The thickness of insulating layer is kept at 10nm for suitable electrical field strength.
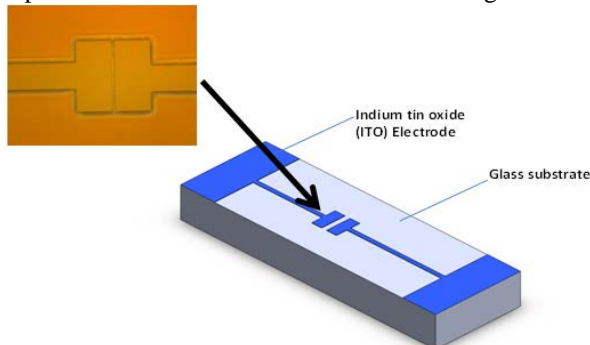
FIGURE 11: 3D model of ITO patterned electrode on top of glass substrate. Two electrodes have a small gap at the center acts as the bottom electrodes. Electrodes at the edge of the glass are for applying suitable electrical signals.

## B. Fabrication of ITO bottom electrode

ITO considered as an ideal transparent metal for viewing particle rotation from an inverted microscope and is hence employed in our work. To fabricate the ITO metal electrode as bottom electrodes, firstly 1 µm thick AZ4562 positive photo-resist layer is coated and patterned by photolithography. Resist is spin coated at the rate of 2000 rpm and soft baked on a hotplate at 95˚C for 50 sec. Later the photo resist is exposed to ultra violate (UV) using a mask aligner. The metal is deposited using a magnetron sputter. Finally unwanted photoresist is stripped off by lift off. Figure 12 shows the MEMS technique process to fabricate bottom electrodes.
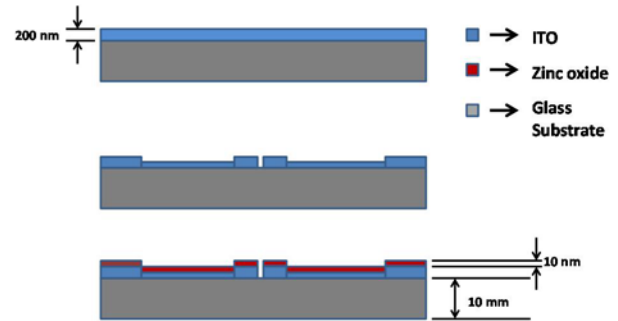
FIGURE 12: Fabrication process of depositing ITO electrode on top of glass substrate. This is one stage of fabrication process.

C. Fabrication of top vertical electrode

The second stage of fabrication involves micro milling 500 micron thick metallic sheet on Perspex. This top portion is then aligned on top of a glass substrate consisting of ITO electrodes. The fabricated micro device is as shown in Figure 13.
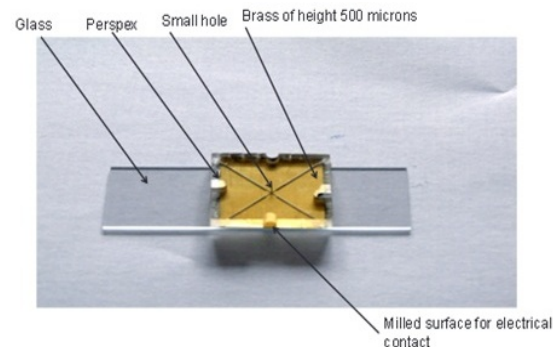

FIGURE 13: Fabricated micro device consisting of top inverted electrodes made of brass are mounted on glass substrate. ITO electrodes are not present in this image.

At the centre of chamber, a high resolution image is shown in Figure 13. Here vertical electrodes and bottom electrodes are in desired position.


(a)   (b)
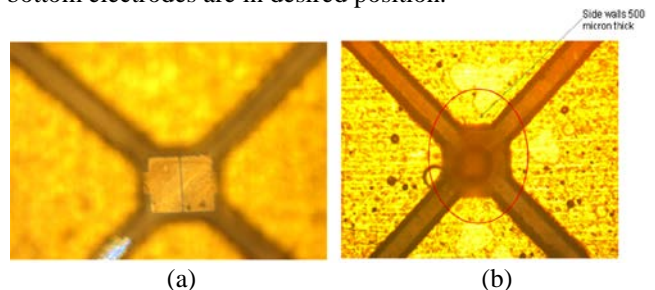
FIGURE 13: Top view of electrode arrangement at the centre chamber. (a) Bottom electrodes are highlighted along with the vertical electrodes. The gap between two pairs of orthogonally arranged electrodes is found to be 750 µm. (b). Side wall vertical electrodes are highlighted in this view. A small hole of 300 µm is also drilled at the center to insert particles or cells.

The grove in between the electrode edges is 350 microns, which is also the micro milling cutter diameter. This cutter is operated at 30,000 rpm cutter spindle speed at the rate of 1.2 µm/s feed rate. Later micro milled part is mated inversely on the ITO metal electrodes. The second stage of fabrication process is as shown in Figure 14.
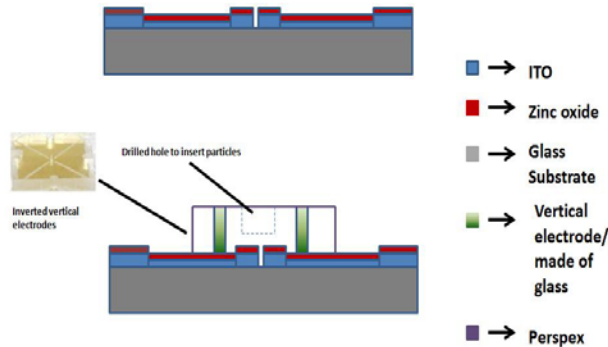
FIGURE 14: Fabrication process of mounting inverted vertical wall electrodes on top of insulated ITO coated glass electrode. Araldite glue is used as the agent to mount the electrodes.

V.   EXPERIMENTAL RESULTS
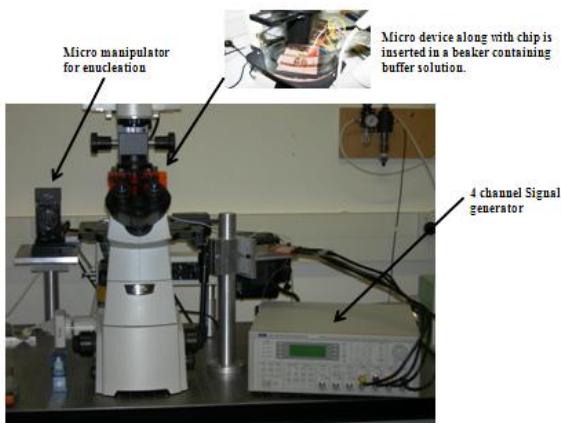
Figure 17: Experimental device setup showing inverted epi-fluorescent microscope along with signal generator assembly.

Figure 17 shows the experimental setup for particle rotation experiments. Setup consists of an inverted epi-fluorescent microscope mounted on anti vibration table. A computer is interfaced with the microscope to capture particle rotation at high resolution. A 4 channel signal generator is available to provide suitable AC signals to the electrodes with phase shifts. A simple chip is fabricated to hold and supply voltage signals to the bottom electrode as shown in Figure 16.
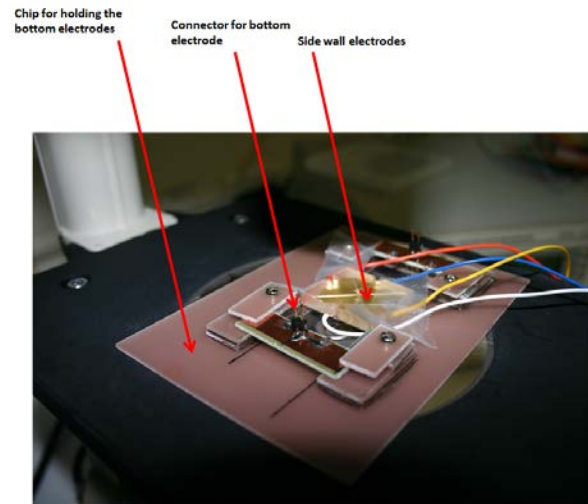
Figure 16: Chip for holding the bottom electrode. The top inverted electrodes are also mounted along with electrical connections.

Materials and Method

The micro device along with fabricated chip is immersed in a beaker containing buffer solution containing 0.85% dextrose and 3% sucrose by weight ratio. 2.65% solid-latex polystyrene beads of 44.16 micron diameter are considered for initial experiments. 1.5 ml polystyrene beads are serially diluted to obtain less than 10 beads. A micro pipette is used to pipette out a single bead. Later a single bead is injected into the rotation chamber as shown in Figure 18.
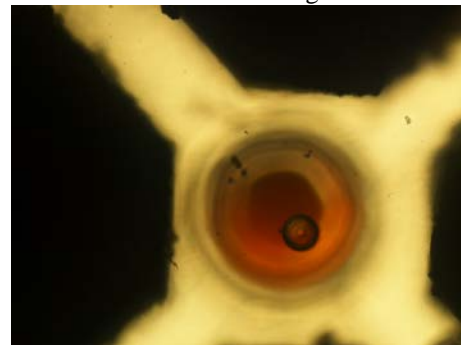
Figure 18: A polystyrene bead is trapped in the rotation chamber for rotation experiments. Bottom electrodes are hidden in this view for clarity.

The polystyrene beads found to be difficult to witness rotation because of the uniformity of the structure. Beads are however seem to be translating in the field. Attached video shows bead movement where more than one beads are suspended in the rotation chamber. Currently the experimental results on polystyrene beads are inconclusive. Bovine cells of 60 micron radius are also processed in the same way as polystyrene beads. The key is to suspend one cell or

particle in the center of chamber with suitable suspending medium. If the specific gravity of water decreases then beads or cells tend to settle at the bottom surface. Currently the experiments are ongoing.

VI.   CONCLUSION

One can achieve 3D rotation by rotating a suspended neutrally charged spherical particle in DEP field. From Euler angles it is evident that two axes of rotation fields are sufficient enough to obtain 3D rotation and control. This DEP field should produce enough torque to rotate the particle. This solely dependent upon the rotational field frequency, complex conductivity and permittivity of particle and surrounding medium, and also on the arrangement of 3D electrodes to generate rotational fields in yaw, pitch and roll axes. Simulation results show that the micro device is capable to produce rotational fields in pitch and yaw in the designed micro device. This is sufficient to obtain all three axes of rotation sequentially in the same rotation chamber. From simulation results it is also evident that the electric fields are linearly super imposed at the center region and is an essential condition to obtain particle rotation. Micro device or biochip is fabricated from the simulated design using photolithography and micro milling technique which is unique and simple. The device is flexible enough to obtain cell rotation, levitation control and moreover it can also be made as open channel by removing the top Perspex which is mounted on brass. This will be very useful while enucleating a cell for high throughput automation. Currently experiments are ongoing with polystyrene and bovine cells. A suitable suspending medium is prepared to suspend particles such as cells. Future works involves carrying out experiments on bovine cells and compare with the simulated data and moreover vision is to simulate a 3D rotating sphere in DEP field.

ACKNOWLEDGMENTS

REFERENCES

1. T. Müller, *et al.*, "A 3-D microelectrode system for handling and caging single cells and particles," *Biosensors and Bioelectronics,* vol. 14, pp. 247-256, (1999).
2. A. Sanchis, A. Brown, M. Sancho, G. Martinez, J. Sebastian, S. Munoz, J. Miranda, Dielectric characterization of bacterial cells using dielectrophoresis, Bioelectromagnetics 28 (5) (2007) 393–401.
3. M. Cristofanilli, G. De Gasperis, L. Zhang, M.-C. Hung, P. Gascoyne, G. Hortobagyi, Automated electrorotation to reveal dielectric variations related to her-2/neu overexpression in mcf-7 sublines, Clinical Cancer Research, 615–619 (2002).
4. T. B. Jones, Electro mechanics of particles. Cambridge; New York; Cambridge University Press, 1995.
5. E. B. Graper, "Charged Particle Flux Generated by an Electron-Beam Deposition Source," *Journal of Vacuum Science & Technology,* vol. 7, pp. 282-, (1970).

6. Morgan, Hywel; Hughes, Michael P.; Green, Nicolas G. "Separation of Submicron Bioparticles by Dielectrophoresis", Biophysical Journal doi:10.1016/S0006-3495(99)76908-0 (volume 77 issue 1 pp.516 - 525)
7. H. B. Li and R. Bashir, "Dielectrophoretic separation and manipulation of live and heat-treated cells of Listeria on micro fabricated devices with Interdigitated electrodes," *Sensor Actuat. B-Chem.*, vol. 86, pp. 215-21, 2002.
8. D.F. Chen, H.Du, W.H.Li, and C.Shu, "Numerical modeling of dielectrophoresis using a meshless approach, " *J.Micromech. Microeng.*, vol. 15, pp. 1040-1048, 2005.
9. R. Pethig , Y. Huang, X. B. Wang, and J.P.H. Burt, "Positive and negative dielectrophoretic collection of colloidal particles using Interdigitated castellated microelectrodes, " *J.Phys. D:Appl. Phys.*, vol. 25, pp. 881-8, 1992.
10. Cell rotation using optoelectronic tweezers Yuan-Li Liang, Yuan Peng Huang, Yen-Sheng Lu, Max T. Hou, and J. Andrew Yeh, Biomicrofluidics.
11. Biedenharn, L. C.; Louck, J. D. (1981), *Angular Momentum in Quantum Physics*, Reading, MA: Addison–Wesley, ISBN 978-0-201-13507-7.
12. Gray, Andrew (1918), *A Treatise on Gyrostatics and Rotational Motion*, London: Macmillan (published 2007), ISBN 978-1-4212-5592-7.
13. J. Gimsa and D. Wachner, "A polarization model overcoming the geometric restrictions of the Laplace solution for spheroidal cells: Obtaining new equations for field-induced forces and transmembrane potential," *Biophysical Journal,* vol. 77, pp. 1316-1326, Sep (1999).
14. H. A. Pohl, *Dielectrophoresis: the behavior of neutral matter in nonuniform electric fields*. Cambridge ; New York: Cambridge University Press, (1978).
15. Thomas B. Jones, "Electromechanics of particles," Cambridge University press, (1995).